Variable Mach Number and AOA Results on Convex Blunt Nose with Five Degree Spike Angle

Srikanth [1], Mahesh [2], Channaveerayya [3]

[1] *Lecturer, Department of Mechanical Engineering, Government Polytechnic Bidar, Karnataka, India.*

[2, 3] *Lecturer, Department of Mechanical Engineering, Government Polytechnic Kalagi, Karnataka, India.*

ABSTRACT

Wave drag is an essential element to consider when constructing high-speed vehicles. Drag may be reduced by altering the flow field in front of the body. There are various approaches for modifying the flow field ahead of a supersonic/hypersonic body, but the employment of a retractable nose spike appears to be the simplest and most efficient way of lowering drag on the vehicle by causing flow separation and altering the shock structure surrounding the body. The current study focuses on high-speed flow around an aero vehicle's blunt nose. Three distinct spike types were investigated for drag reduction research. According to these computer simulations, the right aero will lessen the forces of lift and drag. Data from the literature has been used to validate the numerical results. In light of the simulation findings, alter the blunt nose and spikes to improve aerodynamics, reduce drag, or achieve other design objectives. According to the information provided, an aircraft's front surface can be blunted to provide thermal protection. Despite this blunting, the nose still experiences significant amounts of heat activity, therefore it requires far more thermal protection than the rest of the automobile. Wave drag, which is frequently caused by the blunt nose shape, must be reduced by altering the flow field in front of the vehicle. One way to apply this change is by using a nose spike that retracts. By deploying a retractable spike, the flow field may be altered, potentially reducing wave drag and improving aerodynamic efficiency.

Keywords: Convex Blunt Nose, Spike angle, CFD, Lift and drag forces, AOA, Variable Mach number.

1. INTRODUCTION

Fluid dynamics is the study of fluid flow, or the movement of liquids and gases, within the broader field of fluid mechanics. It encompasses several subfields that study gases in motion, such as aerodynamics and hydrodynamics. Fluid dynamics is used in many activities, including predicting weather patterns, calculating pipeline petroleum flow rates, modeling the explosion of fission bombs, and evaluating airplane forces and moments. Some of its ideas are also applied in traffic engineering, where traffic is viewed as a continuous stream. The theoretical foundation of fluid dynamics, which comprises empirical and semi-empirical laws derived from flow measurement and applied to real-world problems, forms the basis of these applied fields. One popular way to solve a fluid dynamics problem is to calculate the fluid's various properties as functions of location and time, such as temperature, density, pressure, and velocity.

A drag-minimizing When flying at supersonic speeds, the objective of an aero-spike is to reduce blunt body pressure drag. A disconnected shock is produced in front of the body by the aerospike. A zone of recirculating flow forms between the shock and the forebody, reducing drag and creating a more streamlined profile. It is thought that this concept, which was first used to the Trident missile, increased range by 550 kilometers. The Trident aero-spike is an extended boom to which a flat circular plate is affixed. The missile is deployed as soon as it emerges from the submarine and breaks the surface of the sea. The aero-spike allowed for a blunter nose shape, which reduced drag and increased internal room for cargo and propulsion. This was significant because the Trident IC-4 missile, which replaced the Poseidon C-3 missile, has an additional propulsion stage that allowed it to travel farther. The third stage motor had to be positioned in the center of the post-boost vehicle and the reentry vehicles had to be arranged around it in order for it to fit inside the current underwater launch tunnels. When a body is moving, drag is an important factor to take into account. As an automobile accelerates, drag increases. It is the vehicle's resistance to motion brought on by a number of factors. Drag can be grouped based on where it came from. Form drag, profile drag, friction drag, pressure drag, wave drag, and induced drag are a few of them. Only wave drag has been examined here since it is relevant to the case study at hand. Wave drag is the drag force that arises during a shockwave's development.

Wave drag on a body in hypersonic flow is an important aerodynamic consideration. A blunt body with a large nose radius is required to reduce the heating problem, which is most noticeable during the flight's ascent. As a result, the automobile experiences higher wave drag. Reducing wave drag, which is critical in hypersonic flow, would boost propulsive system thrust while decreasing fuel consumption and propulsive system needs, therefore conserving the vehicle's structural integrity and payload capacity. Fuel accounts for more than half of an aircraft's weight, and a 1% decrease in drag increases the vehicle's range or payload capacity by around 10%.

2. LITERATURE REVIEW

literature review on aerodynamic studies using computational techniques for complex flow over the blunt body and aero spikes as a means of reducing drag in subsonic, supersonic, and hypersonic flow. A drag-reducing aero spike is a device designed to reduce the forebody pressure drag of blunt bodies at supersonic speeds. The aero spike creates a separate shock ahead of the body. Between the shock and the forebody, a zone of reticulating flow develops that improves body profile and reduces drag.

Techniques for creating both structured and unstructured meshes are crucial for CFD simulation. Sometimes these methods are combined to create hybrid grids, also known as chimera, composite, or patched grids. Each of these solutions' benefits and drawbacks are covered in this article [1]. Nodes within each cell provide the solution to a flow problem (temperature, pressure, velocity, etc.) in a finite volume formulation. The number of cells in the grid affects a CFD solution's accuracy [2, 20]. Drag is a crucial factor to take into account for a moving body. The amount of drag on a vehicle increases as speed increases. It is the resistance that the vehicle encounters when traveling for a number of reasons. Based on its roots, drag may be categorized into a wide range of areas [3]. A shock wave is produced when a blunt body is in front of a supersonic flow. Because the shock wave begins at an angle to the blunt body's surface, it is known as an oblique shock wave. Fast computers and effective numerical techniques led to the rise in popularity of computational fluid dynamics (CFD) [5, 6, 7]. For fluid dynamics experiments and theory, computational fluid dynamics (CFD) offers a low-cost substitute for real flow simulation. Since it yields good results, the analytically accessible solution has been confirmed to be practical to implement [9]. Therefore, by comparing the numerical results with the available analytical data, one may assess a CFD tool for managing shock capturing difficulties through the use of grid independence studies. A rapid geometry engine (RAGE) has been developed to replace labor-intensive CAD help for early design studies. The geometry tool builds complex aircraft designs using a component-based technique. Basic methods for producing the major components are shown and discussed [18]. A range of fidelity-ranging aerodynamic analysis techniques are applied to a selected geometry model in order to demonstrate the versatility of the geometry tool.

3. COMPUTATIONAL MODEL

To replicate a test case on a digital computer, one must learn enough geometric information about it. With carefully chosen boundaries outside of it to prevent tampering with the physics of the problem, the fluid domain is a fairly defined region of the total system. The fluid around the geometry (external flow issues) is the computational domain in each of the following case studies. Enhancing the shock capturing up to 8–10 times the body width or base diameter is usual in the upstream zone and up to 3–5 times in the remote field.

It should be noted that while all of the current case studies involve outer flow issues, only the fluid domain—and not the solid body—is being represented. Symmetric models are used in the case studies that are being given. The blunt cone body is modeled for flow at zero angle of attack and two non-zero angles of attack (5 degrees and 15 degrees) for both scenarios (without and with spike).

As shown in Figure 1, the ICEM CFD industrial standard code was used to build the 2-D form of a blunt body. Geometric data for blunt bodies with and without spike arrangements are shown in Figure 2. Mesh generation techniques, both organized and unstructured, are essential for CFD simulation. Hybrid grids, often referred to as chimera, composite, or patched grids, are occasionally produced by combining these methods. This article [1] discusses the advantages and disadvantages of each of these strategies

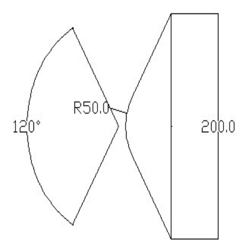

Fig. 1 : Blunt body without spike configuration

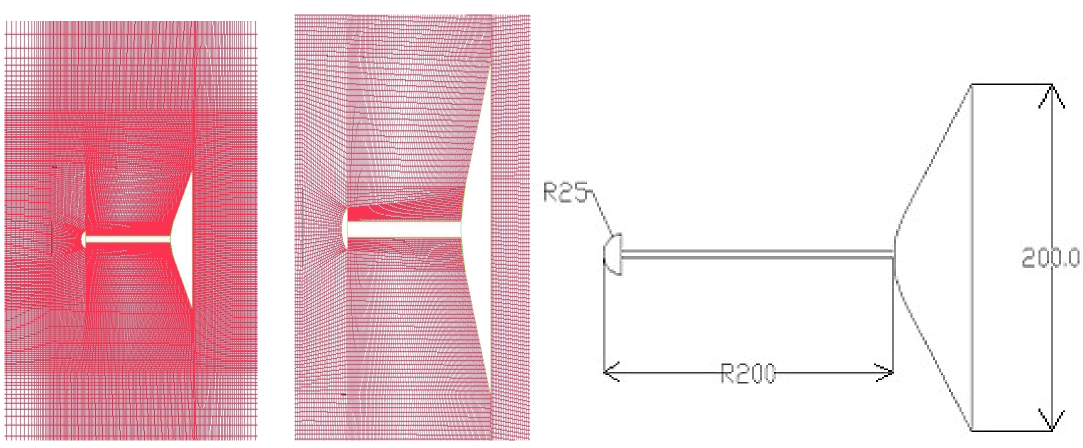

Fig. 2 : Meshed model for Blunt nose, Convex and convex spike configuration

4. PROBLEM STATEMENT

To obtain specific solutions, the fluid must meet the governing equations and the flow geometry constraint and flow field commencing condition must be defined. Therefore, in order to integrate the governing equations, precise measurements of temperature, pressure, and velocity must be made at the region's boundary. When something is transitory, the dependent variable's value at time t=0 must be provided, and the time derivative is of first order. We refer to this as the beginning condition. Additional restrictions placed on the physical boundaries of the fluid area are known as boundary conditions. However, since steady state is presumed in this scenario, no initial conditions are required. Temperature, pressure, and velocity are the usual parameters used to describe the air conditions at an elevation of 5 kilometers (16404 feet) above sea level. It heads toward a subconscious pathway. Every variable in the computational domain is projected to its output from the inner domain. Wall: It is thought that the fluid adheres to the wall because of its viscosity on the blunt body's solid surface. There must be no velocity between the surrounding fluid and the solid, according to the no-slip criterion. Consequently, the fluid is regarded as non-slippery and the wall boundary condition is applied to the blunt cone model surfaces.

The Continuity Equation: $$\frac{\partial \bar{U}_j}{\partial x_j} = 0$$

The Momentum Equation: $$\frac{\partial}{\partial t}(\rho \bar{U}_i) + \frac{\partial}{\partial x_j}(\rho \bar{U}_i \bar{U}_j) = -\frac{\partial \bar{P}}{\partial x_i} - \frac{\partial}{\partial x_j}\left(\bar{\tau}_{ij} + \rho \overline{u_i'' u_j''}\right)$$

The Energy Equation: $$\frac{\partial}{\partial t}(\rho \bar{h}) + \frac{\partial}{\partial x_j}(\rho \bar{U}_j \bar{h}) = -\frac{\partial}{\partial x_j}\left(Q_j + \rho \overline{u_i'' h'}\right)$$

5. CFD RESULTS AND DISCUSSIONS

The convex spike connected to the blunt body in Figures 3 and 4 below exhibits a variety of different forms at zero degrees angle of attachment (AOA) at speeds of 2.0 and 4.0 mach. The distribution of pressure around the blunt body and convex spike is depicted by the pressure contours. A body-fitted shock is said to have produced right before the convex spike. This suggests that the shock wave is rather closely matching the spike's form. It has also been noted that flow separation occurs well at the blunt wall position. If this separation leads to a decrease in the force applied to the blunt wall, aerodynamic drag could be minimized. It is noted that upstream of the spike, the peak pressure contour is captured. This suggests that the compression effects caused by the spike's shape and the incoming flow conditions are likely what led to the location with the maximum pressure. This increased pressure might have an impact on the aerodynamic performance and structural stresses.

5.1 Convex spikes 5 deg AOA and 2.0 Mach

Velocity, Pressure, Density, Temperature Contours & Velocity Vectors, Streamlines plots

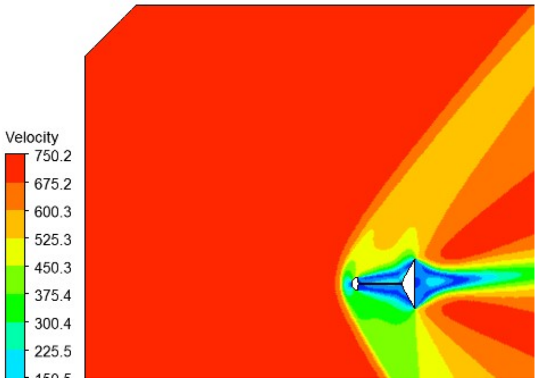

a. Velocity contours

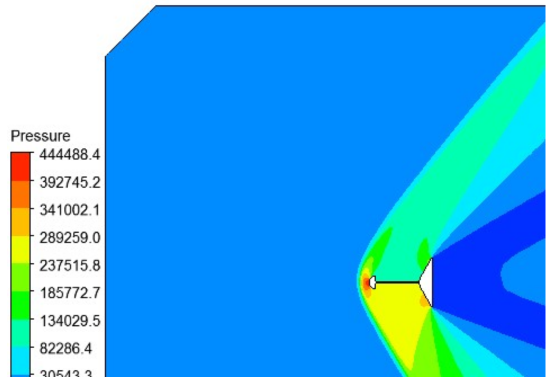

b. Pressure contours

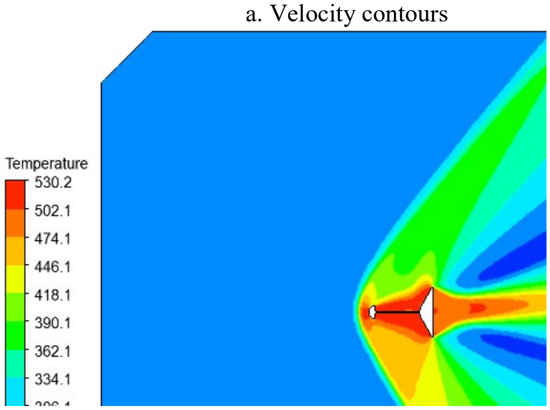

c. Temperature contours

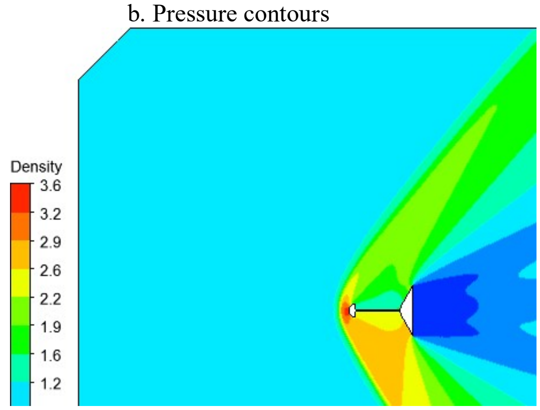

d. Density contours

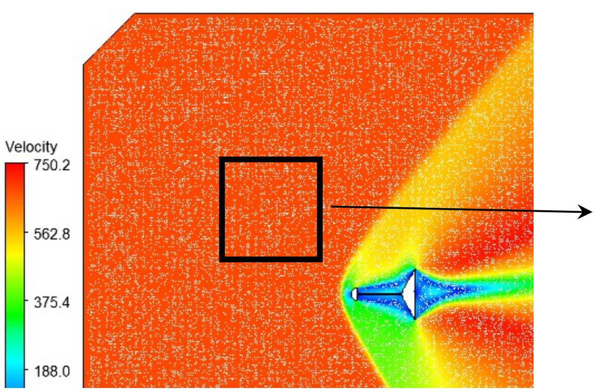

e. Velocity vectors

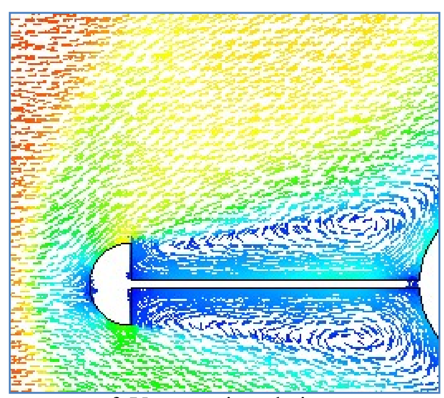
f. Vectors zipped view

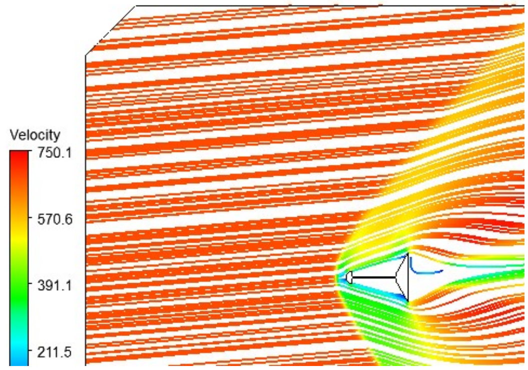

g. Velocity Streamlines

Fig. 3 : Convex spike blunt nose fluid behavior for 2 Mach speed and 5 deg AOA

The above figure displays the various variable contours for the convex spike attached to the blunt body at a 5 degree angle of attack and a speed of 2.0 meters per second. The body-fitted shock has been developed just in front of the convex spike, and the flow has successfully separated at the location of the blunt wall, reducing the force on the blunt wall. It is evident from the pressure fluctuation that the contour's peak pressure is caught at the upstream spike.

Plots of velocity contour patterns have been made for convex spikes with blunt nose bodies. The patterns show that there is a recirculation flow pattern downstream of the blunt body and that there is a shockwave (low velocity zone) upstream of the spike. The shocks are symmetrical in nature.

Figure displays the temperature contour plots for convex spikes and blunt nose bodies. Peak temperature at convex spike is seen. In addition, the temperature is low in the blunt body and high downstream of the spike. As can be observed from the density contour plots for the blunt nose with convex spike in the figure, changes in thermal characteristics cause the peak density to occur at the surface of the spike.

Figure shows the vector plot for the body of the blunt nose. It is evident that until the fluid strikes the convex spikes, its direction and speed remain unchanged. The flow separates and hits the blunt face less frequently as a result of the position spike. The lines of constant value in a stream function are called streamline plots. Figures show that a significant amount of flow recirculation is being caught downstream of the blunt surface.

5.2 Convex spikes 5 deg AOA and 4.0 Mach

Velocity, Pressure, Density, Temperature Contours & Velocity Vectors, Streamlines plots

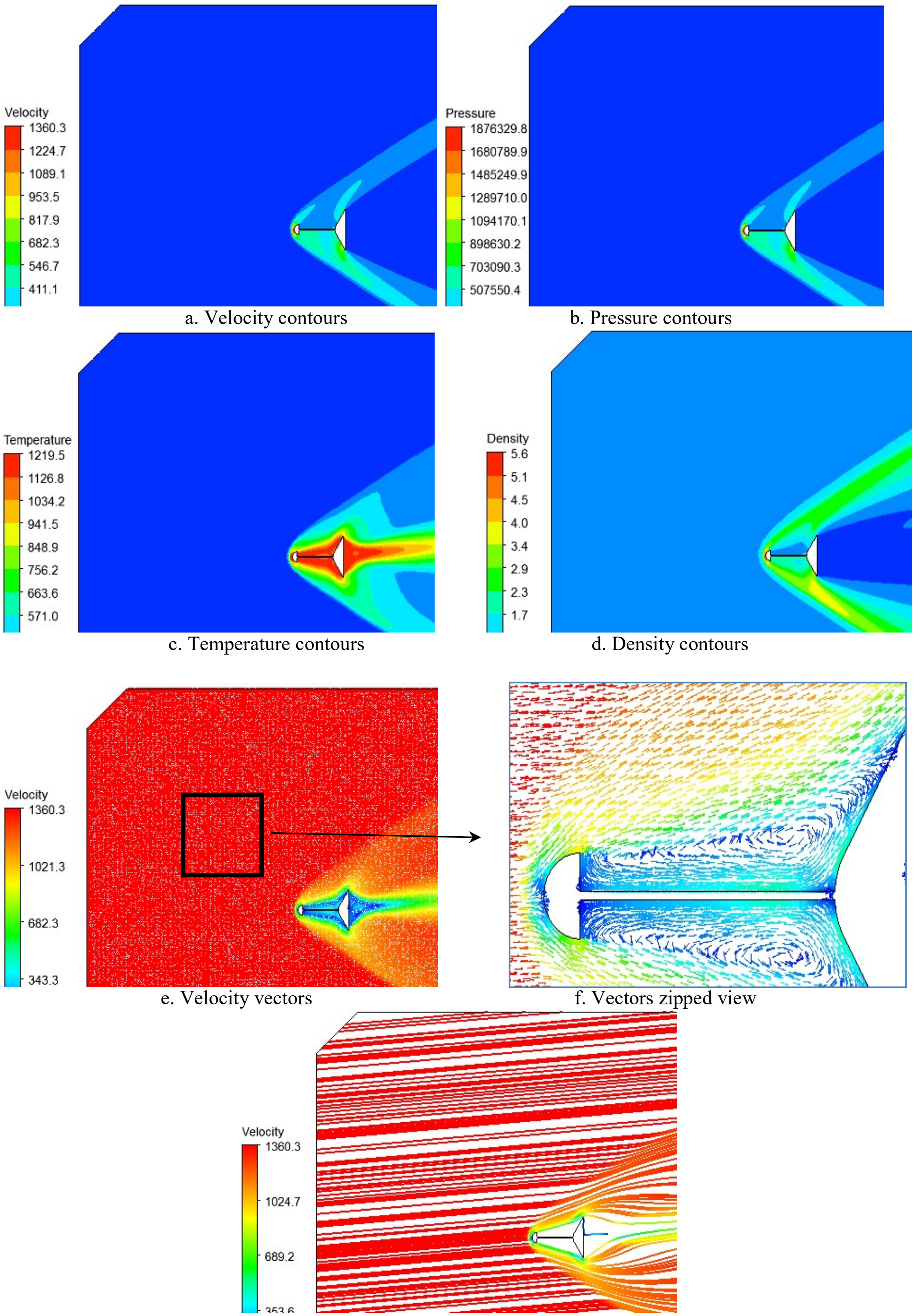

a. Velocity contours
b. Pressure contours
c. Temperature contours
d. Density contours
e. Velocity vectors
f. Vectors zipped view
g. Velocity Streamlines

Fig. 4 : Convex spike blunt nose fluid behavior for 4 Mach speed and 5 deg AOA

The above figure displays the various variable contours for the convex spike attached to the blunt body at 5 degrees AOA and 4.0 meters per second. The body-fitted shock has developed at the point directly in front of the convex spike, and the flow has successfully separated at the location of the blunt wall, reducing the force on the blunt wall. It is evident from the pressure fluctuation that the contour's peak pressure is caught at the upstream spike.

Plots of velocity contour patterns have been made for convex spikes with blunt nose bodies. The patterns show that there is a recirculation flow pattern downstream of the blunt body and that there is a shockwave (low velocity zone) upstream of the spike. The shocks are symmetrical in nature.

Figure displays the temperature contour plots for convex spikes and blunt nose bodies. Peak temperature at convex spike is seen. In addition, the temperature is low in the blunt body and high downstream of the spike. As can be observed from the density contour plots for the blunt nose with convex spike in the figure, changes in thermal characteristics cause the peak density to occur at the surface of the spike.

Vector diagram for convex peaks Figure depicts a body with a blunt snout. It is evident that until the fluid strikes the convex spikes, its direction and speed remain unchanged. The flow separates and hits the blunt face less frequently as a result of the position spike. The lines of constant value in a stream function are called streamline plots. Figures show that a significant amount of flow recirculation is being caught downstream of the blunt surface.

6. CONCLUSIONS

When this spike is affixed to a blunt cone, it successfully relocates the flow re-attachment point away from the model. This is performed by changing the shock structure, which lowers wave drag and drag coefficient. Following an examination of numerous spike designs, it was discovered that the spike with the convex, flat disc-shaped tip had the most potential for minimizing wave drag. This result was calculated using the drag coefficient and the percentage of drag reduction achieved with various spike configurations. The flow field surrounding the blunt body changes depending on the shape of the spike. Moving the re-attachment point away from the model, particularly the convex and flat disc-shaped spike arrangement, was shown to be beneficial in lowering the negative impacts of shock waves on aerodynamic performance. According to the research, modifying the spike design can dramatically lower drag coefficients while increasing the aerodynamic efficiency of the blunt body. The convex and flat disc-shaped spike has significant promise since it can alter the shock structure and minimize wave drag. Taking everything into consideration, your research demonstrates the crucial significance that spike design plays in increasing aerodynamic performance, notably in minimizing wave drag on blunt bodies. Using this knowledge, aerospace vehicle designs might be improved, resulting in an overall gain in efficiency.

REFERENCES

1. Mark Filipiak, Mesh Generation, Version 1.0, Edinburgh Parellel Computing Centre, University of Edinburgh, November-1996.
2. H. K. Versteeg & W. Malasekera, An introduction to Computational Fluid Dynamics-The finite volume method, Pearson Prantice Hall, 1995.
3. John. D. Anderson, Jr, Fundamentals of Aerodynamics, McGraw Hill International Editions, 1985.
4. H W Liepmann & A Roshko, Elements of Gas Dynamics, John Wiley & Sons, Inc. – Galcit Aeronautical series, 1965.
5. John. D. Anderson, "Computational Fluid Dynamics – the basics with applications", McGraw Hill Inc, 1985.
6. Joel. H. Ferziger and Milovan Peric, "Computational Methods for Fluid Dynamics", 3rd revised edition, Springer Verlag publications, 2003.
7. C. A. J. Fletcher, Computational techniques for fluid dynamics – 1, fundamental and general techniques, 2nd edition, 1990.
8. J.F.Thompson, A composite grid generation code for general 3D regions — the Eagle code, AIAA J., Vol. 26 (3) pp.271-272 (1988).
9. S. W. Yuan, "Foundations of fluid mechanics", PHI Publications, 1988.
10. K. Muralidhar & T. Sundararajan, Computational fluid flow and heat transfer, Narosa publishing house, 1984.
11. Pradip Niyogi, S. K. Chakrabartty, M. K. Laha, Introduction to Computational Fluid Dynamics, Pearson Education Series, 2005.
12. S. M. Deshpande & S. V. Raghuramarao, "Numerical methods for compressible flows based on kinetic theory of gases", AR & DB Centre of Excellence for Aerospace CFD, IISc – Bangalore, July 2002.
13. Viren Menezes - PhD thesis, Investigation of aero-spike induced flow field modifications around large angle blunt cone flying at hypersonic mach number, Aerospace Engg Dept, IISc – Bangalore, Feb-2003.
14. K.Sateesh, P.S.Kulkarni, G. Jagadeesh, M. Sun, K. Takayama, Experimental and numerical studies on the use of concentrated energy deposition for aerodynamic drag reduction around re-entry bodies, AIAA, CFD Conference USA.

15. J.S.Shang, Plasma injection for hypersonic blunt body drags reduction, AIAA Journal, Vol.40 No-6, June 2002.
16. K. Satheesh, G. Jagadeesh and P. S. Kulkarni, Hypersonic wave drag reduction in re-entry capsules using concentrated energy deposition, ISSW24, July 12 – 19th, 2004, Beijing, China.
17. Snežana S. Milićev1, Miloš D. Pavlović1, Slavica Ristić2, Aleksandar Vitić2, ON THE INFLUENCE OF SPIKE SHAPE AT SUPERSONIC FLOW PAST BLUNT BODIES, University of Belgrade, Faculty of Mechanical Engineering 27 marta 80, 11000 Belgrade, Yugoslavia
18. David L. Rodriguez* and Peter Sturdza2†, A Rapid Geometry Engine for Preliminary Aircraft Design, Desktop Aeronautics, Inc., Palo Alto, CA, 94301
19. A.N. Volkov a, Yu.M. Tsirkunov a, B. Oesterle b,* Numerical simulation of a supersonic gas–solid flow over a blunt body: The role of inter-particle collisions and Two-way coupling effects, International Journal of Multiphase Flow 31 (2005) 1244–1275
20. Timothy, Baker. Mesh generation: Art or science? MAE Department, Princeton University, Princeton, NJ 08540, USA
21. S. P. Kuo1, “Shock Wave Modification by a Plasma Spike: Experiment and Theory”, Department of Electrical & Computer Engineering, Polytechnic University, 6 MetroTech Center, Brooklyn, NY 11201, USA. Received October 14, 2004; accepted November 9, 2004